This is a “preproof” accepted article for *Mineralogical Magazine*.

This version may be subject to change during the production process.

10.1180/mgm.2024.93

REVISION I

Dervillite from Jáchymov, Czech Republic: a non-harmonic approach to the refinement of atomic displacement parameters of silver

JAKUB PLÁŠIL[1*], EMIL MAKOVICKY[2], VÁCLAV PETŘÍČEK[1] AND PAVEL ŠKÁCHA[3]

[1] Institute of Physics of the CAS, v.v.i., Na Slovance 1999/2, 18200 Prague 8, Czech Republic

[2] Department of Geosciences and Resource Management, University of Copenhagen, Østervoldgade 10, DK-1350, Copenhagen K, Denmark

[3] Department of Mineralogy and Petrology, National Museum, Cirkusová 1740, Prague 9 - Horní Počernice, 193 00, Czech Republic

*Corresponding author; Email: plasil@fzu.cz

Abstract
A rare silver mineral, dervillite (ideally Ag_2AsS_2), has been found in specimens from the famous Jáchymov mining district, Czech Republic. It occurs as very rare long-prismatic crystals up to 0.4 mm across in association with proustite, bismuth and native silver in the thin arsenic veinlets within the Trojická vein (Svornost mine). Dervillite is monoclinic, space group *Pc*, with a = 9.6375(3), b = 12.9462(4), c = 6.8497(2) Å, β = 99.510(2)°, and V = 842.88(2) Å^3 (Z = 8). The new structure refinement, R_1 = 2.94% for 18767 reflections with [$I > 3\sigma(I)$] and wR_2 = 7.93% for all 20050 reflections, provided a better fit to the data, compared to earlier studies, revealing that silver (8 symmetrically independent atomic sites), which adopts for various coordinations (from quasi-linear to tetrahedral) in the structure of dervillite vibrates non-harmonically at room temperature. The Gram-Charlier development, describing the atomic displacement parameters of silver atoms, was used to model their non-harmonic behavior. A discussion on the use of the approach to the data with limited quality is provided as well.

Keywords: dervillite, silver mineral, crystal structure, Gram-Charlier refinement, non-harmonicity, Jáchymov deposit.

Introduction
Dervillite, Ag_2AsS_2, has been described for the first time from the famous Sainte-Marie-aux-Mines mining district in Vosges (Haut-Rhine Province, France) by Weil (1941) as a mineral consisting of Pb, S and Sb, and also possibly of Bi, with a later reinvestigation by Bari et al. (1983). A complete structural study had to wait for more than seventy years. Bindi *et al.* (2013) published the complete structure refinement for dervillite based on the single-crystal X-ray diffraction data obtained from a crystal found in the famous Lengenbach quarry in Wallis, Switzerland.

We have reinvestigated dervillite structure on a crystal from Jáchymov (Czech Republic), paying special attention to the silver atoms and the description of their atomic displacement parameters, respectively, in detail. Here, we report on employing the Gram-Charlier development to silver's atomic displacement parameters in the dervillite structure.

New occurrence of dervillite from Jáchymov deposit, Czech Republic
Dervillite was found in the material originating from old workings in the Sv. Trojice, or also Trojická (Holy Trinity) vein, in the vicinity of the crosscut with the Geschieber vein at the

Daniel level of the Svornost mine, Jáchymov ore district, Krušné Hory Mts, Czech Republic. Jáchymov ore district is a world-famous locality for about 450 mineral species and a historically important district of Ag + As + Co + Ni + Bi and of U vein-type mesothermal mineralization (Škácha *et al.*, 2019). The ore veins cut a complex of medium-grade metasedimentary rocks of Cambrian to Ordovician age in the envelope of Variscan granite plutons. Most ore minerals were deposited during Variscan mineralization from meso thermal fluids (Ondrus et al. 2003a, 2003b). The complex geochemistry of primary mineralization led to an unusually rich supergene zone, with occurrences of numerous minerals formed during post-mining processes (Ondruš *et al.*, 1997; Škácha *et al.*, 2019).

Seven ore stages were distinguished within the Jáchymov ore field: Sn-W sulfoarsenide, ore-free quartz, carbonate–uraninite, arsenide, arsenic-sulfide, sulfide and post-ore stage. Economically, the most important was the carbonate–uraninite stage for uranium ores and the arsenic-sulfide for silver ores. The Trojická vein is one of the typical constituents of the oldest Sn-W sulfoarsenide stage. This stage is related to the auto-metamorphism of younger granite, which underlies the whole district and has no relation to the younger five-element mineralization (Ondruš *et al.*, 2003b).

Mineralization with currently studied dervillite was identified in several ore vein fragments. The mineral was found in up to 2 cm thick vein of native arsenic, which is locally brecciated, enclosing the tiny fragments of mica-schists. The oldest mineral in the association is skeletal or fine-grained native silver in aggregates up to 5 mm, sometimes naturally etched from native arsenic. Arsenic also encloses rare small cubes of violet fluorite. Rare cavities host thick pyramidal dark red proustite crystals in size up to 2 mm, very rarely associated with dervillite. Black prismatic dervillite crystals with strong metal luster up to 0.5 mm occurred only rarely. It replaces proustite with usually fine-grained native bismuth, which further replaces both mentioned minerals. Supergene arsenolite forms up to 2 mm large octahedra or their aggregates and covers the rock fragments containing native arsenic. It also sometimes forms fillings of fractures.

Chemical composition

Chemical analyses of dervillite and closely associated proustite were performed using a Cameca SX100 electron microprobe operating in wavelength-dispersive mode (20 kV, 20 nA, and 1 μm beam size). The following standards and X-ray lines were used to minimize line overlaps: Ag (Ag*L*α), Bi (Bi*L*α), Bi_2Se_3 (Se*L*β), Cd (Cd*L*α), chalcopyrite (Cu*K*α, Fe*K*α, S*K*α),

FeAsS (As*K*β), HgS (Hg*L*α), NaCl (Cl*K*α), PbS (Pb*M*α), Sb_2S_3 (Sb*L*β), Sn (Sn*L*β) and ZnS (Zn*K*α). Peak counting times were 20 seconds for all elements and 10 seconds for each background. Cadmium, Fe, Pb, Bi, Ni, Co, Au, Se, Sn, and Zn were found to be below the detection limits (0.01–0.05 wt%). Raw intensities were converted to the concentrations of elements using the automatic "PAP" (Pouchou and Pichoir, 1985) matrix-correction procedure.

With the exception of Cl and Te contents slightly above the detection limits, only antimony and copper enter both phases' structures, from which Cu preferentially enters the dervillite structure and Sb enters the proustite (Table 1), which tightly accompanies by dervillite on the studied specimen.Analytical data for dervillite (12 analyses) and proustite (8 analyses) are given in Table 1. Based on 5 *apfu*, the empirical formula for dervillite from Jáchymov is $Ag_{1.97}Cu_{0.05}As_{1.01}S_{1.96}$. On the basis of 7 *apfu*, the empirical chemical formula for the studied proustite closelz associated with dervillite is $Ag_{3.03}(As_{0.99}Sb_{0.01})_{3.00}S_{2.95}Cl_{0.01}$.

Single-crystal X-ray diffraction

Dervillite crystal of the approximate dimensions 0.128 × 0.038 × 0.014 mm was examined at room temperature using a Rigaku SuperNova single-crystal diffractometer. The diffraction experiment was done using Mo*K*α radiation (λ = 0.71073 Å) from a micro-focus X-ray tube collimated and monochromatized by mirror-optics and detected by an Atlas S2 CCD detector (2×2 pixels binning). According to single-crystal X-ray data dervillite is monoclinic, the *P*-centered unit cell: *a* = 9.6375(3), *b* = 12.9462(4), *c* = 6.8497(2) Å, β = 99.510(2)°, with *V* = 842.88(2) $Å^3$ (Table 2). Corrections for background, Lorentz, polarization effects, and absorption correction were applied during data reduction in the *CrysAlis* (Rigaku, 2024) package.

Structure refinement proceeded in the Jana2020 program (Petříček *et al.*, 2023), employing the model of Bindi *et al.* (2013). Following the previous structure determination, dervillite has been found to crystallize in a non-centrosymmetric monoclinic space-group *Pc* (Table 2). The refined Flack parameter, 0.169(7), is very similar to the configuration of the structure studied by Bindi *et al.* (2013). Crystal structure refinement that included all atoms refined with anisotropic displacement parameters returned very acceptable *R*-values: R_1 = 3.41% for 18767 reflections with $I > 3\sigma(I)$ and wR_2 = 8.70 for all 20050 reflections with a *goodness-of-fit* of 1.76 for all reflections. Nonetheless, several difference-Fourier maxima ($\Delta\rho_{max}$ = 1.87 e $Å^{-3}$) remained undescribed after the final refinement cycle. They all were found to be close to the

silver atoms; the highest of them was localized 0.92 Å from Ag6. Inspection of the difference-Fourier maps showed that this remaining electron density, connected with the silver atoms, cannot be described by the simple harmonic approach to the atomic displacement parameters. Therefore, the non-harmonic displacement parameters were implemented for refinement and were modeled as the Gram-Charlier third-order development (see, e.g., Volkov *et al.*, 2023) of the *ADP*s. At the initial stage, all the Ag atoms were considered and checked carefully for the significance of the variable changes (as $\Delta(param)/\sigma(param)$). Only those atoms with a significant contribution of the non-harmonicity to the atomic displacement were considered in the final model. We employed Wilson's correction to prevent statistical bias in the least-squares refinement (Wilson, 1976). The final refinement, including all Ag atoms refined with non-harmonic atomic displacement parameters, converged to the R_1 = 2.94% for 18767 reflections with $I > 3\sigma(I)$ and wR_2 = 7.93 for 20050 reflections with a *goodness-of-fit* of 1.61 for all reflections and $\Delta\rho_{max}$ = 0.77 e Å^{-3}. The experimental and refinement details for both harmonic and non-harmonic approaches are reported in Table 2. Atomic parameters, including non-harmonic terms (Gram-Charlier development), are embedded in the CIF file. Selected interatomic distances calculated from the refined model are provided in Table 3. Programs Jana2020 (Petříček *et al.*, 2023) and Vesta3 (Momma and Izumi, 2011) were used to plot the electron density and the isosurface for Ag atoms' atomic displacement parameters (ADPs).

General description of the crystal structure

Despite its simple chemical formula, in agreement with its low symmetry, the crystal structure of dervillite contains eight independent silver positions, four distinct arsenic sites, and eight different sulfur sites.

The dervillite structure is divided into thick (010) slabs with a complex internal structure. The (010) planar gaps separate the slabs, which are bridged over and interconnected only by Ag–S bonds; these bind together the planar slab surfaces. Perpendicular to this scheme and conspicuous in the [001] projection, the structure is formed by (100)-oriented Ag-predominant portions with wavy character (these are layers with a complex configuration, Figs. 2 and 3), which alternate with continuous (100) interlayers distinguished by the predominant role of lone-electron pairs of arsenic (Figs. 2, 3, and in detail Fig. 5). In most cases, the longe-electron-pairs (*LEP*s) interact with opposing Ag atoms, resulting in lone-electron-pair micelles of unusual type. In their (100) interlayer, adjacent micelles are separated by short intervals containing Ag–S bonds (Fig. 3, 5). The shortest Ag–Ag contacts

observed in the structure, of about 3 Å in length, are limited to the Ag-concentrating layers (Fig. 6a), whereas the short, strong As–As bonds are situated in the surfaces of the *LEP*-based interlayers (detailed view in Figs 5a, b).

The sub-sulfide character of dervillite (Bindi *et al.*, 2013) is thus demonstrated by a combination of As–As bonding, involvement of Ag in interactions with *LEP*s of As, and by at least one example of weak cation-cation (i.e., Ag–Ag) interaction. In the As–As pair, the covalent bond consumes two electrons, and the As–As group functions as two divalent cations. With 4 Ag *pfu* added, the charge of four S^{2-} becomes compensated.

Ag-based polyhedra

The bulk of silver atoms comprises nearly tetrahedral coordination, mostly with additional complications or variations.

Ag1 and Ag5 are tetrahedra, with all four corners occupied by sulfur (Table 3). Bond lengths vary between 2.556 Å and 2.665 Å, exceptionally reaching 2.700 Å. There is an additional Ag–Ag contact at 3.096 Å between Ag1 to Ag6. The Ag3 is a tetrahedron with three sulfurs and one As/Sb as vertices (Figs. 3 and 6b).

Ag2 is [3]-coordinated near-to-planar arrangement by three S atoms (S3 and 2× S7) and additionally by one bond to As1/Sb1 (via *LEP*) and an Ag–Ag contact Ag5 (3.216 Å), forming a distorted tetragonal bipyramid (including Ag) or trigonal pyramid (including just As/Sb coordination). Ag4 is a tetrahedron with all ligands represented by S atoms.

Ag6 is in a trigonal planar configuration (S2, S6, S8; 2.43–2.83 Å) with an additional Ag–Ag contact to Ag1 (3.097 Å). Ag7 is also in trigonal coordination by three S atoms (S3, S4, S5; 2.41–2.86 Å) plus two Ag–Ag contacts: to Ag5 (3.188 Å) and Ag8 (3.016 Å). Ag8 is a pseudo-linear configuration, plus a side-bond to Ag7 (3.016 Å) that completes a triangle. A close contact to Ag3 (3.174 Å) should be also mentioned here, on the opposite side from Ag7. The linear-disposed S–Ag–S bonds are 2.394 Å and 2.428 Å.

Arsenic

All arsenic atoms in the structure are paired by a covalent bond, with As–As distance between 2.493 Å and 2.506 Å (Figs 5a, b, c). In the weaker As–As interactions range, As2 and As3 more or less face one another with their *LEP*s (Fig. 5b). Bindi *et al.* (2013) noted that As1 and As4 face and react with the opposing Ag atoms. Apparently, the *LEP*s of arsenic and orbitals of Ag react (always as an As–Ag pair, one by one) and reduce the As–Ag distance to

only 2.716 Å or slightly above this value. The Ag–As interaction via *LEP*s of arsenic (donation to the Ag orbitals, see Bindi *et al.*, 2013) is comparable to the 2.65 Å long Cu–*LEP*(As) interaction in spaltiite $Cu_2Tl_2As_2S_5$ (Graeser *et al.*, 2014, illustrated in Makovicky, 2018) which also contains modified *LEP* micelles which remind of those in the present structure. The short covalent As–As bonding present in dervillite deserves comparison with other similarly behaving subsulfides such as mineral lautite, CuAsS (Bindi *et al.*, 2008) (As–As = 2.4965(8) Å), the As–S molecular compounds (e.g., dimorphite: 2.46–2.48; realgar: 2.56–2.57; pararealgar: 2.48–2.53 Å, uzonite: 2.50–2.58 Å; see Bonazzi and Bindi, 2008; wakabayashilite: 2.656 Å, Bonazzi *et al.*, 2005), with complex sulfosalt sterryite (2.63 Å; Moëlo *et al.*, 2012), or even with the covalently bonded As in the structure of arsenic (Wyckoff, 1963; As–As = 2.506 Å). As Bindi *et al.* (2013) pointed out, the weak Ag–As bonds in dervillite, of the dative-donation character of bond (As lone pair to the closed-shell d^{10} Ag cations, secure a kind of an '*anionic*' character of the dervillite structure.

S-based tetrahedra

Regarding sulfur-centered coordination polyhedra, S-based tetrahedra are the principal polyhedral element of the crystal structure of dervillite (Fig. 4). Among the sulfur atoms, S1, S4, S5, S6, S7 and S8 are in tetrahedral coordination by 3 Ag + 1 As. These tetrahedra are all flattened by the central S atom being shifted towards the triangular Ag_3 base, which opposes the short S–As bond (the only one of the short As–S bonds per S atom). Unlike these six sulfur-centered polyhedra, the S2 site is in a square pyramid with As as the apical vertex (4 Ag + 1 As), and S3 in an octahedron formed by 5 Ag + 1 As. As2 and As3 more or less face one another with their *LEP*s, whereas As1 and As4 face, and *via* their *LEP*s react with the opposing Ag atoms (always as a pair As–Ag). The regular presence of one As-S bond in every coordination polyhedron of S is typical for dervillite and demonstrates evenness of local charge compensation throughout the structure.

Structural adjustments to the sub-sulfide character

An exciting aspect of the dervillite structure is a conversion of the As–S–As distance to As–As distance by "weakening the As–S interconnections" The average As–As bond in dervillite is 2.5 Å long whereas the average As–S distance is approximately 2.24 Å. Thus, the "full-sulfide" As–S–As distance of 4.48 Å will be reduced to 2.5 Å, *i.e.*, with a loss of 1.98 Å. The directions in question are diagonal to the *b* parameter so that the length loss on the *b* dimension can be estimated at approximately 1.5 Å or more (Figs. 2, 3, 5a,c).

Looking at the position of As–As vectors in the structure (e.g., Fig. 2), they are situated in the (100) planes and centered on y = 0.25 and 0.75. Furthermore, especially the As–Ag interactions define a general herringbone orientation of bonds, which is also expressed in a wavy character of (100) layers (Fig. 2). *LEP* micelles are oriented diagonally in the (010) layers, right and left of the composition planes, which separate adjacent (010) layers.

As an example of a configurational situation, the (100) face of the *LEP* micelle is formed by Ag3 in tetrahedral coordination and Ag5 in triangular coordination. They are joined by S4, which tops the mentioned face. In the Ag-rich wavy (100) layer, they are followed by Ag6 and Ag8, which are differently coordinated. What is essential is that the two such configurations with converging arrangement/orientation force Ag7 into a linear [001] arrangement, the only linear chain of silver. Ag6 and especially Ag8 are coordinated by S3 positioned on the (-100) face of the next *LEP* micelle along the [100] direction, and then the configuration repeats itself.

The just mentioned (010) composition plane, which amalgamates the herringbone-arranged blocks (at y = 0.5, with centrally positioned Ag7, and limited by Ag1–Ag1 positions), differs from that at y = 0.0, which lacks a centrally situated Ag atom and is limited by Ag2–Ag2 and Ag3–Ag3 [100] sequences (Fig. 2). Thus, the alternating composition planes differ from one another. The *c*-glide planes are situated in these planes of slab contacts.

Discussion - Non-harmonic *vs.* Harmonic refinement

Recently, a thorough discussion on the use of harmonic *vs*. non-harmonic atomic displacement parameters has been provided by Plášil et al. (2024). The authors also commented in detail on the careful evaluation and handling of the experimental data. It is essential to adequately consider how much "*non-harmonicity*" could be used in the refinement, i.e. up to which order of the Gram-Charlier development we can opt for and use. In the current case, we have decided to keep only the third-order for all the Ag atoms, keeping in mind that the data quality (resolution) is still somewhat limited (for instance, compared to the case of the recently investigated mineral theuerdankite, described by Plášil *et al.*, 2024). The use of a non-harmonic approach of the *ADP*s of all Ag atoms in dervillite provided much cleaner (and also meaningful) difference Fourier maps (compare Figs. 7a and 7b), although the drop in the *R*-values is not the "rocket" one. Vast of the Ag atoms behave/vibrate in the same fashion in the structure of dervillite, but to a greater or lesser extent. Generally, the atoms vibrate perpendicular to the actual bonds (Ag–S) (Fig 8). The effect of the non-

harmonicity is namely apparent for Ag7 and Ag8 atoms (Fig. 8a-c). Noteworthy, from the *j.p.d.f.* (*joint-probability-density function*) maps, it seems that the Ag3–Ag8 interaction might be more favored than for Ag7–Ag8, despite the distances for the first mentioned pair being somewhat longer (3.17 for Ag for the Ag3–Ag8 *vs.* 3.01 Å for Ag7–Ag8). None of the silver atoms at room temperature is highly mobile in dervillite; nevertheless, all silver atoms in the dervillite structure are "non-harmonically vibrating". The non-harmonic refinement of all Ag atoms in the structure of dervillite led to a reasonable and better model-to-data fit. The improvement is not apparent at first glance from the quick drop of *R*-values, but it is obvious from the difference-Fourier maps. We can expect greater Ag mobility at higher temperatures, namely for the Ag7–Ag8 join (maybe Ag3?) (check particularly Fig. 8c). However this should be a subject for the subsequent temperature-dependent diffraction study.

Acknowledgements. The helpful comments of principal editor Stuart Mills, and two anonymous referees are greatly appreciated. This study was supported by project TERAFIT - CZ.02.01.01/00/22_008/0004594 (JP and VP). Additionally, we acknowledge the support by the Ministry of Culture of the Czech Republic (long-term project DKRVO 2024-2028/1.II.a; National Museum, 00023272) for PS.

Supplementary material. The supplementary material for this article can be found at .....

Competing interests. The authors declare none.

References

Bari, H., Cesbron, F., Moëlo, Y., Permingeat, F., Picot, P., Pierrot, R., Schubnel, H.J., and Weil, R. (1983) La dervillite, Ag_2AsS_2, nouvelle définition de l'espèce. *Bulletin de Minéralogie*, **106**, 519–524.

Becker, P.J. and Coppens, P. (1974) Extinction within the limit of validity of the Darwin transfer equations. I. General formalism for primary and secondary extinction and their applications to spherical crystals. *Acta Crystallographica*, **A30**, 129–147.

Bindi, L. and Evain, M. (2007) Gram-Charlier development of the atomic displacement factors into mineral structures: The case of samsonite, $Ag_4MnSb_2S_6$. American Mineralogist, 92, 886-891.

Bindi, L., Catelani, T., Chelazzi, L. and Bonazzi, P. (2008) Reinvestigation of the crystal structure of lautite, CuAsS. *Acta Crystallographica*, **E64**, i22.

Bindi, L., Nestola, F., De Battisti, L. and Guastoni, A. (2013) Dervillite, Ag_2AsS_2, from Lengenbach quarry, Binn valley, Switzerland: occurrence and crystal structure. *Mineralogical Magazine*, **77**, 3105–3112.

Bonazzi, P. and Bindi, L. (2008) A crystallographic review of arsenic sulfides: Effects of chemical variations and changes induced by light exposure. *Zeitschrift für Kristallographie*, **223**, 132–147.

Bonazzi, P., Lampronti, G.I., Bindi, L., and Zandari, S. (2005) Wakabayashilite, $[(As,Sb)_6S_9][As_4S_5]$: crystal structure, psuedosymmetry, twinning, and revised chemical formula. *American Mineralogist*, 90, 1108–1114.

Graeser, S., Topa, D., Effenberger, H., Makovicky, E. and Paar, W.H. (2014) Spaltiite, IMA 2014-012. CNMNC Newsletter No. 20, June 2014, page 557; *Mineralogical Magazine*, **78**, 549–558.

Laufek, F., Sejkora, J. and Dušek, M. (2010) The role of silver in the crystal structure of pyrargyrite: single-crystal X-ray diffraction study. Journal of Geosciences, 55, 161–167.

Makovicky, E. (2018) Modular Crystal Chemistry of Thallium Sulfosalts. *Minerals*, **8**(11), 478.

Moëlo, Y., Guillot-Deudon, C., Evain, M., Orlandi, P., and Biagioni, C. (2012) Comparative modular analysis of two complex sulfosalt structures: sterryite, $Cu(Ag,Cu)_3Pb_{19}(Sb,As)_{22}(As\text{-}As)S_{56}$, and parasterryite, $Ag_4Pb_{20}(Sb,As)_{24}S_{58}$. *Acta Crystallographica*, **B68**, 480–492.

Momma, K., and Izumi, F. (2011) VESTA 3 for three-dimensional visualization of crystal, volumetric and morphology data. *Journal of Applied Crystallography*, **44**, 1272–1276.

Ondruš, P., Veselovský, F., Skála, R., Císařová, I., Hloušek, J., Frýda, J., Vavřín, I., Čejka, J. and Gabašová, A. (1997) New naturally occurring phases of secondary origin from Jáchymov (Joachimsthal). *Journal of the Czech Geological Society*, **42**, 77–108.

Ondruš, P., Veselovský, F., Gabašová, A., Hloušek, J., Šrein, V., Vavřín, I., Skála, R., Sejkora, J. and Drábek, M. (2003a) Primary minerals of the Jáchymov ore district. *Journal of the Czech Geological Society*, **48**(3-4), 19–147.

Ondruš, P., Veselovský, F., Gabašová, A., Hloušek, J., Šrein, V., (2003b): Geology and hydrothermal vein system of the Jáchyrnov (Joachimsthal) ore district. *Journal of the Czech Geological Society*, **48**(3–4), 3–18.

Petříček, V., Palatinus, L., Plášil, J. and Dušek, M. (2023) Jana2020 - a new version of the crystallographic computing system Jana. *Zeitschrift für Kristallographie*, **238**(7–8), 271–282.

Plášil, J., Sejkora, J., Dolníček, Z., Petříček, V., Désor, J., Majzlan, J., Gross, M., Möhn, G. and Schürmann, Ch. (2024) Theuerdankite, Ag_3AsO_4, a new mineral from the Alter Theuerdank Mine (St. Andreasberg), Germany. Mineralogical Magazine. Published online 2024:1-21. doi:10.1180/mgm.2024.44.

Pouchou, J.L., and Pichoir, F. (1985) "PAP" (πρZ) procedure for improved quantitative microanalysis. *In* J.T. Armstrong, Ed., Microbeam Analysis, p. 104–106. San Francisco Press, California.

Rigaku (2024) CrysAlis CCD and CrysAlis RED. Rigaku- Oxford Diffraction Ltd, Yarnton, Oxfordshire, UK.

Škácha, P., Plášil, J., and Horák, V. (2019) Jáchymov: mineralogická perla Krušnohoří. Academia, Praha 682 pp. (in Czech with the English summary)

Volkov, S. N., Charkin, D. O., Firsova, V. A., Aksenov, S. M. and Bubnova, R. S. (2023) Gram–Charlier approach for non-harmonic atomic displacements in inorganic solids: A review, Crystallography Reviews, 29, 151–194.

Wilson, A.J.C. (1976) Statistical Bias in Least-Squares Refinement. *Acta Crystallographica*, **A32**, 994–996.

Weil, R. (1941) La dervillite, espèce minérale nouvelle. Revue des Sciences Naturelles d'Auvergne 7, 110–111.

Wyckoff, R.W. (1963) Crystal Structures 1, Second Edition, Interscience Publisher, pp. 7–83.

FIGURE CAPTIONS

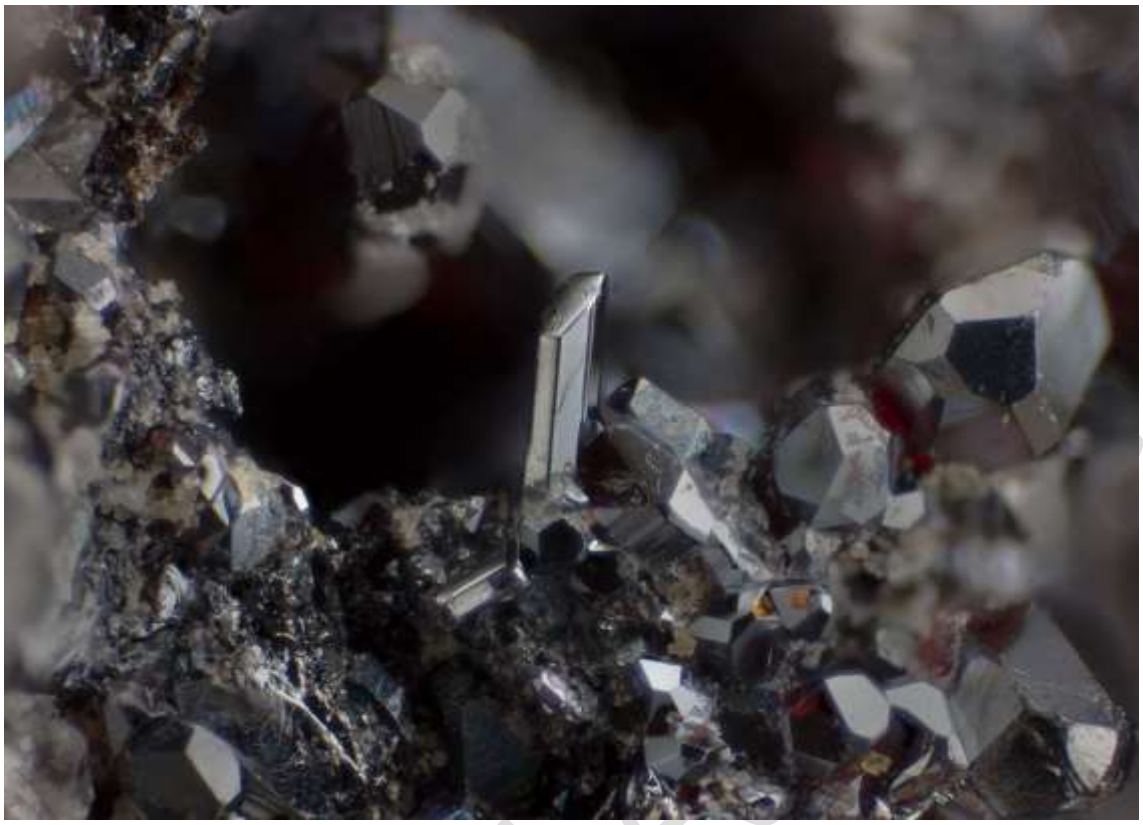

Figure 1. Dervillite prismatic crystal (~0.4 mm across) associated with multifacted proustite crystals from Jáchymov. Photo by P. Škácha.

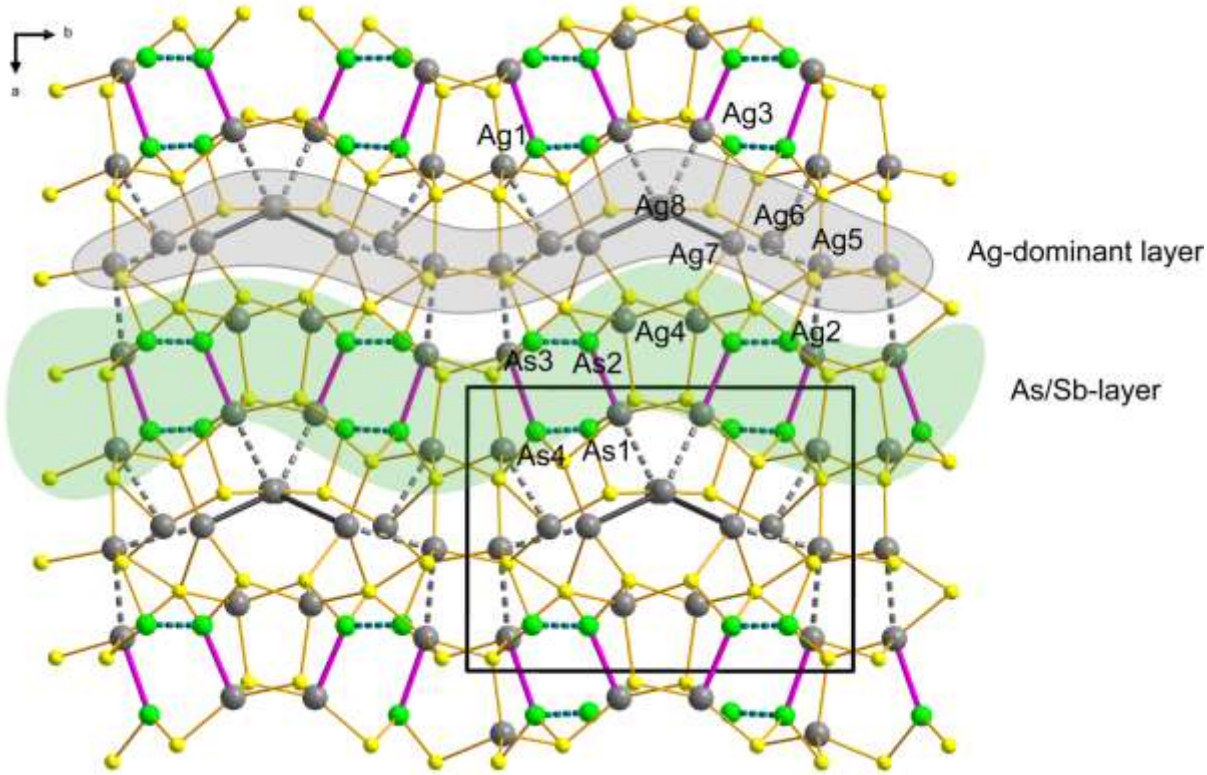

Figure 2 Crystal structure of dervillite viewed down **c** approximately (slightly inclined) in the *ball-and-stick* presentation. S: yellow; Ag: dark grey, As: green. Cation pairs As–As (dashed

teal-colored line representing covalent bond), Ag–As (purple-colored interaction of lone-electron pair of As with Ag), and Ag–Ag (grey-colored joins representing metal-metal interactions; dashed grey lines indicate close metal-metal contacts: Ag1–Ag6 = extra sheet contact, Ag3–Ag8 = extra sheet contact, Ag5–Ag7, Ag7–Ag8) in dervillite. Unit-cell edges outlined in black solid lines.

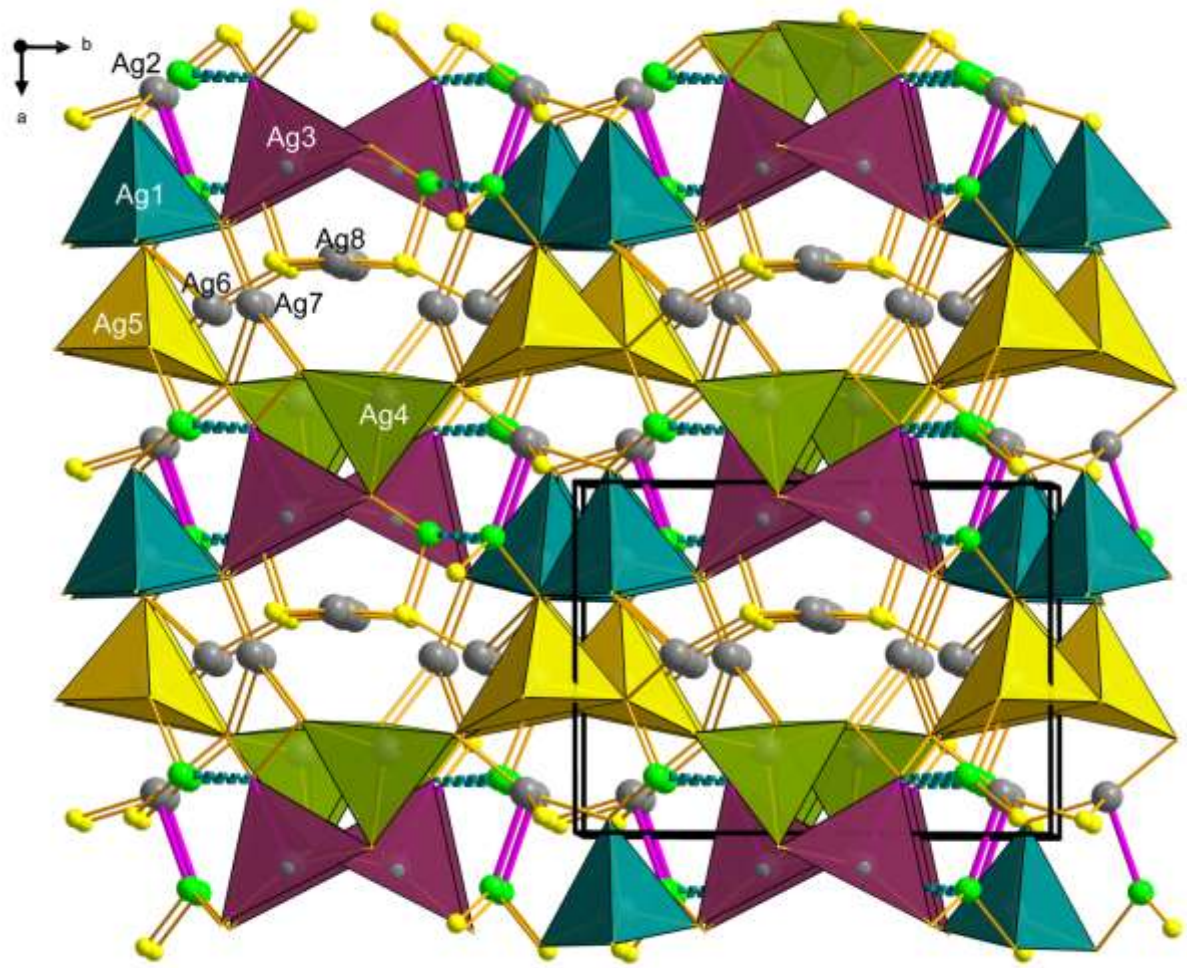

Figure 3 Projection of the crystal structure of dervillite along **c**, showing coordination of silver atoms. Tetrahedrally coordinated: Ag1, Ag3, Ag4, Ag5; triangular coordination Ag2, Ag6, Ag7, Ag8. Dashed lines represent As–As (*LEP*s), violet solid lines Ag–As interactions.

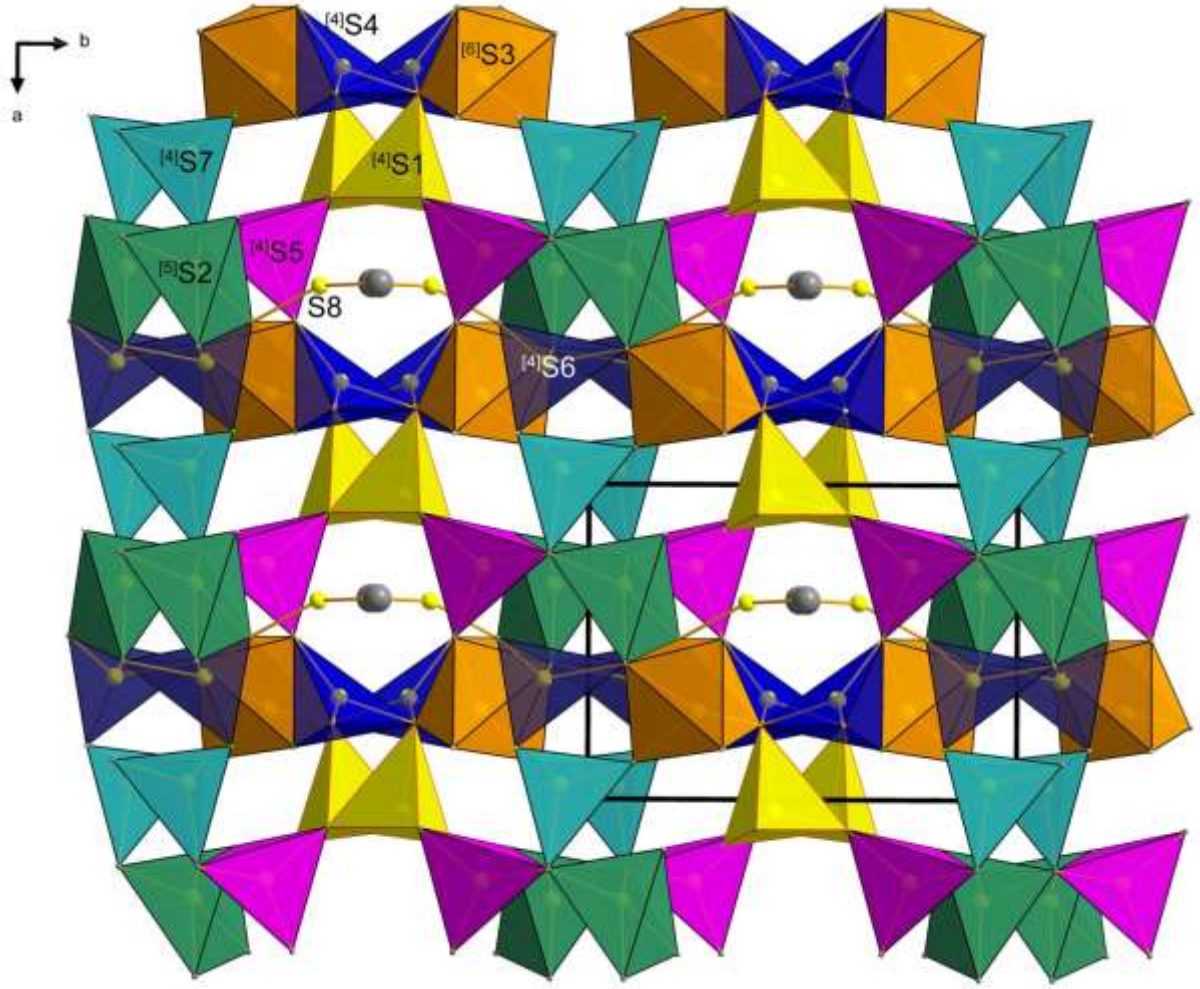

Figure 4 S-based polyhedra in the crystal structure of dervillite. Polyhedra for S8 atom is omitted for clarity of the picture, but it is [4]-coordinated (As4, 2×Ag8, Ag6). Cation–cation interactions are omitted for clarity as well.

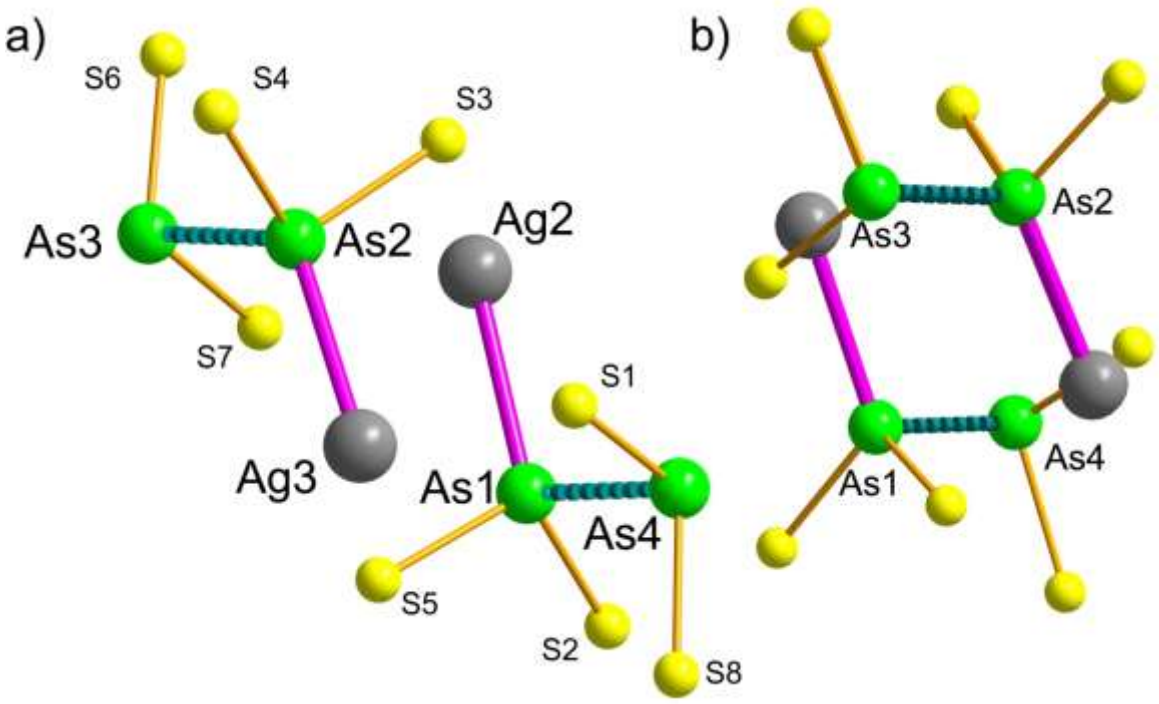

Figure 5 The *LEP*-bonded arsenic–silver slab from the crystal structure of dervillite with Ag intercalations. **A)** A side-view on As–As pairs and their bonding environments. **B)** The view is perpendicular to the previous one with overlapping As–As joins and *LEP* micelles

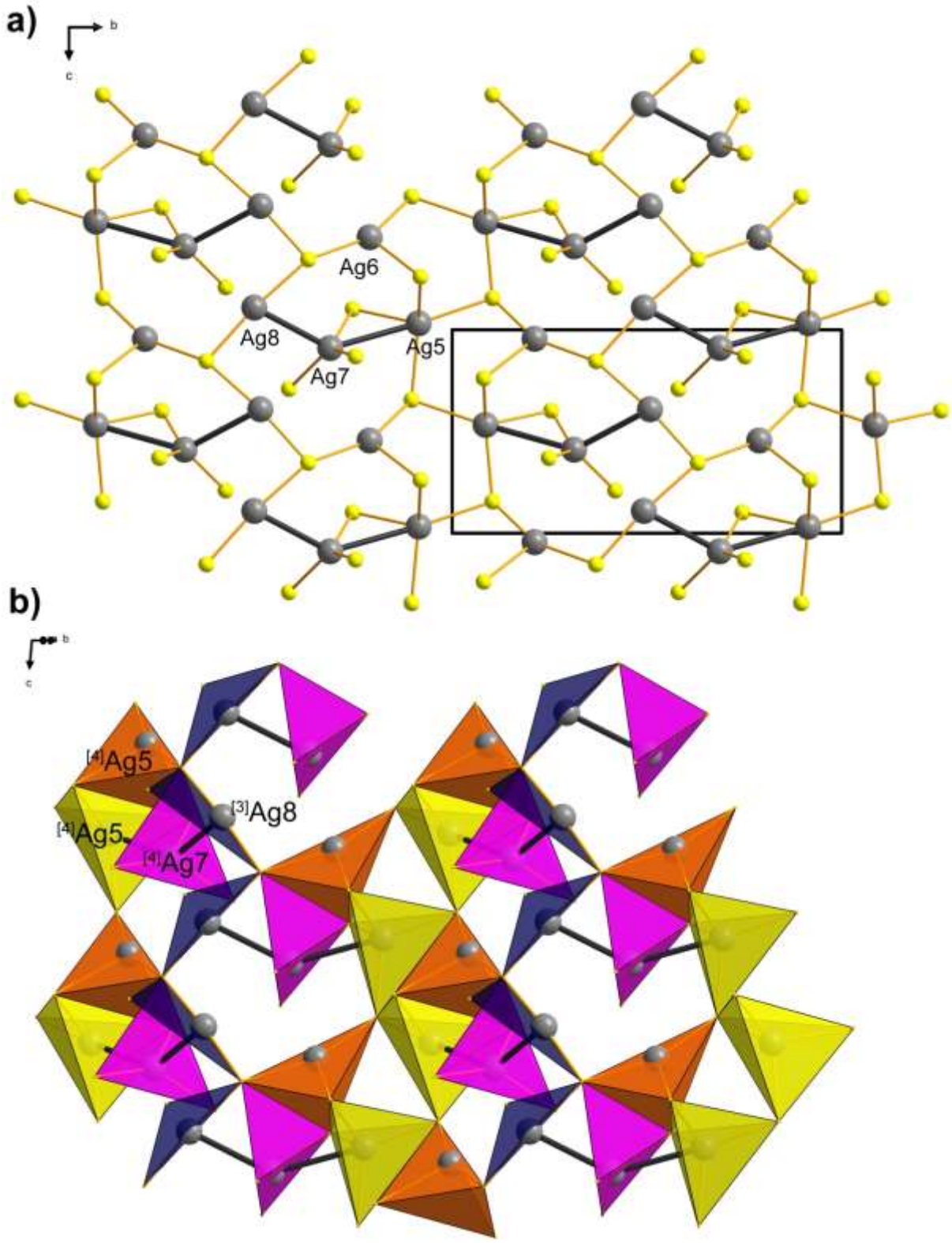

Figure 6 The complex silver-rich wavy (100) layer from the crystal structure of dervillite: **a)** Ball-and-stick model, **b)** polyhedral model. Ag1, Ag2, Ag3 and Ag4 are not present within this layer. The dark-grey bond represents Ag–Ag interactions.

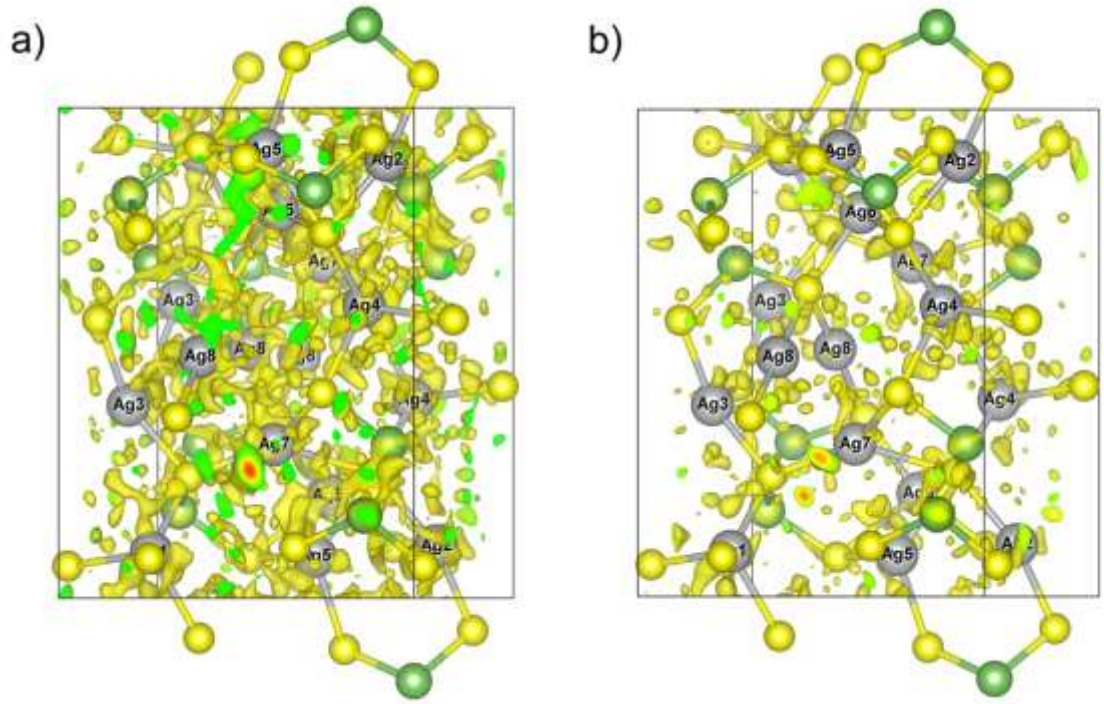

Figure 7 Difference-Fourier 3D maps plotted for the entire unit cell of dervillite. **A)** Harmonic vs. **b)** non-harmonic refinement. The isosurface level is set to the same value (0.25).

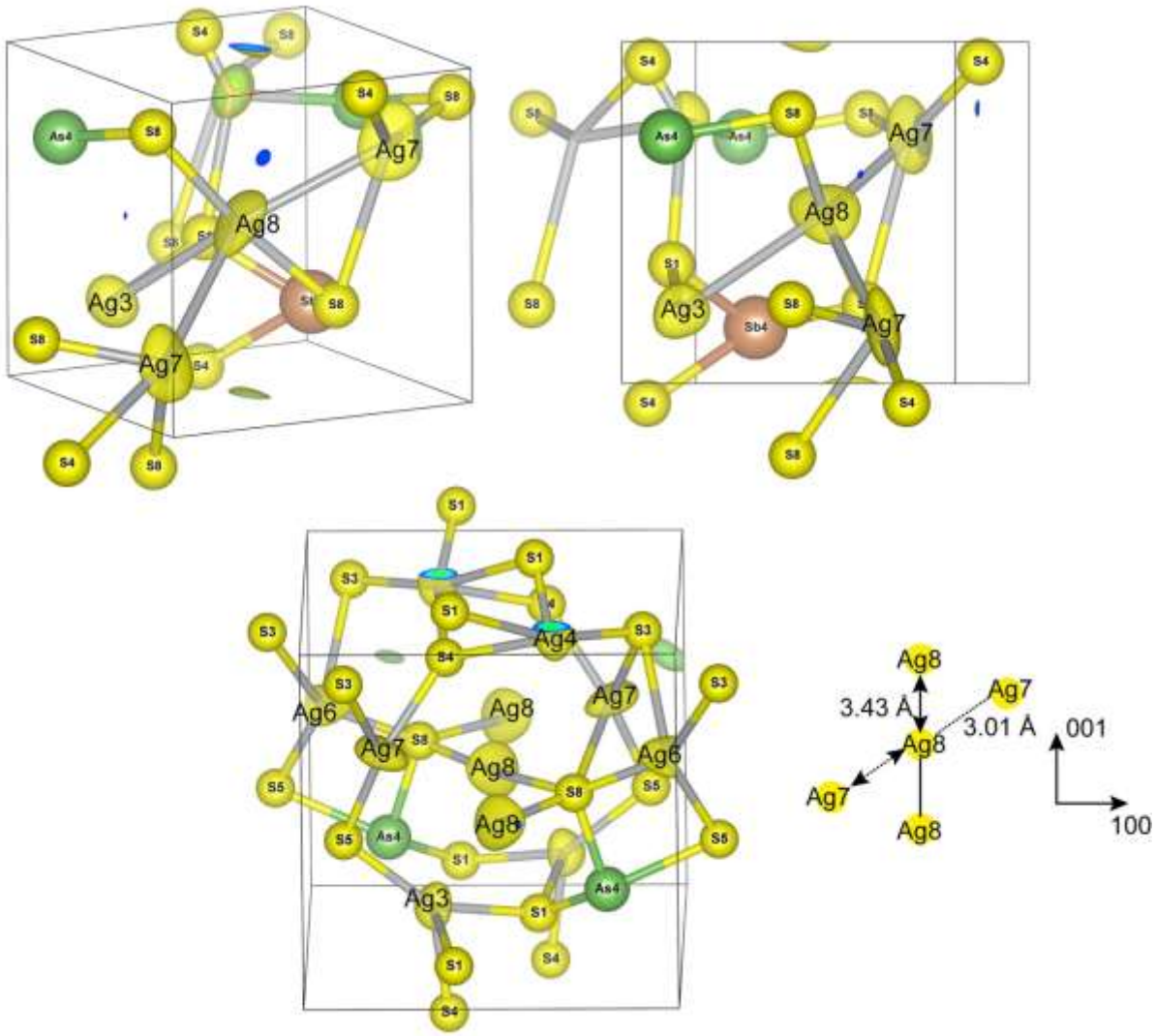

Figure 8 Three different projections providing a view of the non-harmonic atomic displacement parameters of Ag in the structure of dervillite (represented by the *j.p.d.f.* isosurface). The metal-metal interactions are displayed as dark-grey joins, and the size of the S, As/Sb atoms is set arbitrarily. Noteworthy is a pseudo-linear arrangement of the Ag8–Ag8 atoms in the structure (extending along c) and "diagonally" arranged interacting Ag7 atoms (approximately in a plane). The highest mobility of the silver (diffusion) could be expected there at non-ambient temperatures. The joint probability density function calculations by Jana2020 and plotted by Vesta3. The isosurface level of the 3D maps is 0.05 $Å^{-3}$.

TABLE CAPTIONS

Table 1. Chemical composition (in wt.%) for dervillite (n = 12) and proustite (n = 8) from Jáchymov as determined by electron microprobe (WDS).

		Mean	Range	St.Dev.
Dervillite	Ag	58.99	58.52–59.89	0.38
	Cu	0.86	0.80–0.93	0.04
	As	21.00	20.81–21.31	0.18
	Te	0.07	0.00–0.11	0.04
	S	17.48	17.34–17.66	0.11
	Cl	0.03	0.00–0.08	0.03
Proustite	Ag	64.85	64.51–65.21	0.26
	Sb	0.21	0.00–0.74	0.26
	As	14.76	14.39–14.96	0.18
	Te	0.07	0.00–0.13	0.05
	S	18.75	18.63–18.93	0.09
	Cl	0.06	0.00–0.08	0.02

Table 2. Summary of data collection and refinement for dervillite from Jáchymov.

	Harmonic refinement	Non-harmonic refinement
Structural formula (sum)	$Ag_2(As_{0.973}Sb_{0.027})S_2$	$Ag_2(As_{0.976}Sb_{0.024})S_2$
a, *b*, *c* [Å], β [°]	9.637(2), 12.946(3), 6.850(2), 99.51(3)	
V [Å^3]	842.9(4)	
Space group	*Pc*	
Z	8	
$D_{calc.}$ [g.cm^{-3}] for the above formula	5.612	5.608
Temperature		
Wavelength	MoK_α, 0.71073 Å	
Crystal dimensions	128 × 38 × 14 μm	
Limiting θ angles (Completeness to θ_{max})	2.66°–28.07° (97%)	
Limiting Miller indices	$-12 \le h \le 12$, $-16 \le k \le 17$, $-8 \le l \le 9$	
No. of reflections measured	20084	20084
No. of unique reflections	20050	20050
No. of observed reflections (criterion)	18767 [I_{obs}>3σ(I)]	18767 [I_{obs}>3σ(I)]
Absorption correction (mm^{-1})	17.806	17.811
F_{000}	3331	1275
Culled reflections ([I_{culled}>20σ(I)])	34	34
Parameters refined, restraints, constraints	187, 0, 38	267, 0, 38
R, wR^2 (obs)	0.0341, 0.0848	0.0294, 0.0774
R, wR^2 (all)	0.0362, 0.0870	0.0312, 0.0793
GOF obs/all	1.77/1.76	1.62/1.61
$\Delta\rho_{min}$, $\Delta\rho_{max}$ (e Å^{-3}); max. charge (e)	–1.35/1.87 (0.92 Å to Ag6), 0.58	–0.40/0.54 (0.87 Å to Ag4), 0.25
Weighting scheme,	σ, w = 1/[σ^2(F_o^2)+(0.02P)^2], P	σ, w = 1/[σ^2(F_o^2)+(0.02P)^2], P

weights	$= (F_o^2+2F_c^2)/3$	$= (F_o^2+2F_c^2)/3$
Extinction coeff. (B-C type, Becker and Coppens, 1974)	226(13)	262(12)
Flack parameter	0.166(7)	0.169(7)

Table 3. Selected interatomic distances (in Å) in dervillite from Jáchymov.

Ag atoms					
Ag1–S2	2.597(2)	Ag4–S1^{iv}	2.672(2)	Ag7–S3^{v}	2.855(2)
Ag1–S2^{i}	2.6415(19)	Ag4–S3^{iv}	2.5934(18)	Ag7–S4^{v}	2.521(2)
Ag1–S5	2.6375(18)	Ag4–S4	2.553(2)	Ag7–S5	2.411(2)
Ag1–S7	2.581(2)	Ag4–S4^{ix}	2.6221(19)	Ag7–Ag8	3.016(2)
Ag1–Ag6	3.0976(19)				
		Ag5–S2	2.644(2)	Ag8–S8	2.429(2)
Ag2–S3^{ii}	2.5181(19)	Ag5–S3^{xiv}	2.701(2)	Ag8–S8^{ix}	2.394(2)
Ag2–S7	2.5065(19)	Ag5–S6^{xiv}	2.556(2)	Ag8–Ag8^{viii}	3.431(3)
Ag2–S7^{ii}	2.646(2)	Ag5–S6^{xv}	2.664(2)		
Ag2–As1/Sb1^{ii}	2.7996(16)	Ag5–Ag7^{iv}	3.188(2)		
Ag3–S1	2.591(2)	Ag6–S2	2.831(2)		
Ag3–S1^{ix}	2.4793(19)	Ag6–S6^{v}	2.433(2)		
Ag3–S5	2.4928(19)	Ag6–S8^{iv}	2.504(2)		
Ag3–As2/Sb2	2.7159(15)				
As/Sb atoms					
As1/Sb1–As4	2.4942(12)	As2/Sb2–As3	2.5054(12)	As3/Sb3–S6	2.2477(18)
As1/Sb2–S2^{iii}	2.2418(17)	As2/Sb2–S3	2.2480(18)	As3/Sb3–S7	2.2155(17)
As1/Sb3–S5	2.2362(18)	As2/Sb2–S4	2.2539(17)		
				As4/Sb4–S1	2.2189(17)
				As4/Sb4–S8	2.2788(17)

Symmetry codes: (i) *x*, –*y*+2, *z*–1/2; (ii) *x*, –*y*+2, *z*+1/2; (iii) *x*, *y*, *z*–1; (iv) *x*, *y*, *z*+1; (v) *x*+1, *y*, *z*; (vi) *x*–1, *y*, *z*–1; (vii) *x*–1, –*y*+2, *z*–1/2; (viii) *x*, –*y*+1, *z*–1/2; (ix) *x*, –*y*+1, *z*+1/2; (x) *x*–1, *y*, *z*; (xi) *x*–1, *y*, *z*+1; (xii) *x*–1, –*y*+1, *z*+1/2; (xiii) *x*, –*y*+1, *z*+3/2; (xiv) *x*+1, *y*, *z*+1; (xv) *x*+1, –*y*+2, *z*+1/2.